

CO₂ absorption with diamine functionalized deep eutectic solvents in microstructured reactors



Mohsin Pasha^a, Hong Zhang^a, Minjing Shang^a, Guangxiao Li^a, Yuanhai Su^{a,b,*}

^a School of Chemistry and Chemical Engineering, Frontiers Science Center for Transformative Molecules, Shanghai Jiao Tong University, Shanghai 200240, PR China

^b Key Laboratory of Thin Film and Microfabrication (Ministry of Education), Shanghai Jiao Tong University, Shanghai 200240, PR China

ARTICLE INFO

Article history:

Received 6 September 2021

Received in revised form 21 November 2021

Accepted 20 December 2021

Available online 25 December 2021

Keywords:

CO₂ capture

MAPA functionalized DES

Viscosity

Microstructured reactor

Process intensification

ABSTRACT

Deep eutectic solvents (DESs) have gained much attention to capture CO₂ nowadays because of their simpler synthesis, higher sustainability and better eco-friendly properties compared to ionic liquids and conventional amine sorbents. Herein, we analyzed the CO₂ absorption performance of five novel diamine functionalized DESs in microstructured reactors (MSRs) with metal foams as packing materials. Interestingly, the DES functionalized with N-methyl-1,3-propanediamine (MAPA) showed remarkable absorption performance without significant viscosity rise. The CO₂ loading and absorption efficiency of this DES could reach 0.78 mol of CO₂ / mol of diamine and 98% at the gas to liquid flow rate ratios of 640 and 240, respectively. Even computational studies showed that the ethylenediamine (EDA) functionalized DES had the highest CO₂ uptake ability due to the low energy barrier, but sudden rise in viscosity of the EDA functionalized DES reduced its CO₂ absorption ability compared to the MAPA functionalized DES. Further experiments indicated that the MAPA functionalized DES showed low heat of absorption and remarkable regeneration ability. Overall rate constant and absorption flux of this DES were higher than most previously used amine functionalized DESs. Consequently, the unification of this remarkable DES and microreactors has great process intensification potential for CO₂ absorption.

© 2021 Published by Elsevier B.V. on behalf of Institution of Chemical Engineers.

1. Introduction

Thriving concentration of carbon dioxide (CO₂) in the atmosphere has become one of serious concerns in current era. Gigatons of CO₂ are emitted into the atmosphere every year (Lim, 2015; Vishwakarma et al., 2017), leading to serious environmental ramifications, such as global warming, rising sea level (Uma Maheswari and Palanivelu, 2015) and reduction in crop production (Sun et al., 2017). Amine-based sorbents have been used in industry for several decades, yet having several technological issues, such as corrosion, sorbent degradation, high energy penalty for regeneration, and so on. These shortcomings in conventional amine sorbents provide a gateway to greener and sustainable sorbents for CO₂ capture (Altamash et al., 2016; Dutcher et al., 2015). Ionic liquids (ILs) have been widely applied for CO₂ capture in the last two decades, and exhibited great CO₂ uptake ability with remarkable characteristics, such as high thermal stability, negligible vapor pressure and tunable structures (Aghaie et al., 2018; Nguyen and Zondervan, 2018; Ramdin et al., 2012b). However, synthesis of a task specific IL for

CO₂ capture needs deep understanding and knowledge of its structure-property relationship at molecular scale, which is a painstaking and time-consuming process. Furthermore, ILs have several additional drawbacks, such as complex synthesis protocol, escalating cost, poor biodegradability and so on (Aghaie et al., 2018; Ramdin et al., 2012a).

Deep eutectic solvents (DESs) are considered to be sustainable and eco-friendly sorbents for CO₂ capture. They belong to a subclass of ILs and are typically synthesized by mixing quaternary ammonium salt containing halide anion, such as choline chloride (ChCl) that acts as hydrogen bond acceptor (HBA), with amines, carboxylic acid or alcohol that serves as hydrogen bond donor (HBD). Such resulting solutions have low melting temperatures due to charge delocalization through hydrogen bonding interaction between HBA and HBD (Abbott et al., 2004; Carriazo et al., 2012; Hansen et al., 2021; Sarmad et al., 2017; Zhang et al., 2012). The terms DES and IL are mutually used in literature as both liquids have common properties, such as low vapor pressure and high thermal stability. However, DESs are normally formulated with Lewis and Bronsted acids and bases that contain multiple cationic and anionic species rather than discrete ionic species used in the formulation of ILs (Smith et al., 2014). Moreover, DESs have several advantages over ILs, such as lower cost of raw materials, simpler synthesis, higher biodegradability, and less potential of by-product formation showing their

* Correspondence to: Department of Chemical Engineering, School of Chemistry and Chemical Engineering, Shanghai Jiao Tong University, Shanghai 200240, PR China.

E-mail address: y.su@sjtu.edu.cn (Y. Su).

ecofriendly nature (Sarmad et al., 2017). Because of these phenomenal features, DESs containing CO₂-philic moieties, such as amine and carboxylic acid in HBA or HBD, are widely used for CO₂ capture.

Amine and superbase functionalized DESs have been used in several studies relating to CO₂ capture. For instance, Sze et al. (2014) synthesized five superbase functionalized DESs by using ChCl as HBA and glycerol as HBD. The DES functionalized with 1,5-diazabicyclo [4.3.0]-non-5-ene (DBN) exhibited the highest CO₂ uptake ability among these involved DESs. Yan et al. (2020) formulated three superbase functionalized DESs by using superbase IL as HBA and ethylene glycol (EG) as HBD. Among these DESs, the DES that was composed of 1,8-diazabicyclo-[5.4.0]undec-7-ene imidazole [HDBU] [Im] and EG with a mass ratio of 7:3 showed the greatest CO₂ uptake ability of 0.141 g of CO₂/g of DES. Trivedi et al. (2016) prepared an amine functionalized DES by using monoethanolamine hydrochloride salt as HBA and ethylenediamine (EDA) as HBD. This DES had outstanding CO₂ uptake ability due to simultaneous functionalization of HBA and HBD with the amine moiety. Recently, Sarmad et al. (2020) synthesized six amine functionalized DESs by using ChCl as HBA and ethanolamine as HBD, and five different additional amines were respectively used for the functionalization. The piperazine (PZ) functionalized DES showed the best CO₂ absorption performance among these DESs.

In order to enhance the process efficiency for CO₂ capture, it is of viable strategy to apply advanced reactor technologies. It has been highlighted in several reports that the CO₂ absorption rate in microreactors is significantly higher than conventional absorbers because of their larger specific interfacial area and faster transport rate (Ganapathy et al., 2014; Guo et al., 2019; Ma et al., 2020). Additionally, high CO₂ uptake ability of some amine and superbase functionalized DESs was reported in several investigations by using pure CO₂ as feed gas (Trivedi et al., 2016; Zhang et al., 2019). However, the CO₂ content in flue gases released from the coal fired power plants is found in the range of 12–15% (v/v) (Drage et al., 2012). For the CO₂ absorption in amine and superbase functionalized DESs using continuous-flow microreactors, the biggest hindrance is the drastic rise in the viscosity with the progress of CO₂ absorption. This effect becomes more exacerbated with the solidification of carbamate, leading to the clogging of microreactors.

Herein, we present five novel diamine functionalized DESs composed of ChCl and EG as HBA and HBD with molar ratio of 1:4 and modified with different additional diamines, including hexamethylenediamine (HMDA), aminoethylethanamine (AEEA), N-methyl-1,3-propanediamine (MAPA), ethylenediamine (EDA) and 1,4 butanediamine (BDA) for CO₂ absorption in the microstructured reactors with metal foams as packing materials. The gas to liquid flow rate ratio was varied from 240 to 640 to comprehensively analyze the CO₂ uptake ability of these DESs and figured out the clogging potential of MSRs. Moreover, computational studies were performed to examine the interaction between amine (-NH₂) and CO₂ by analyzing N-C bond length and O-C-O bond angle in these DESs. Various parameters such as molar ratio of EG to diamine, temperature and water content were studied to better study the absorption performance of these DESs. Regeneration and kinetic investigations were performed to indicate the recyclability potential and CO₂ absorption rates of these DESs. Finally, comparison of MSRs with other microreactors was executed to demonstrate the potential improvement made by these diamine functionalized DESs at high gas to liquid flow rate ratios.

2. Experimental Section

2.1. Materials

Hexamethylenediamine (HMDA, purity 99%), aminoethylethanamine (AEEA, purity 99%), N-methyl-1,3-propanediamine

(MAPA, purity 98%), ethylenediamine (EDA, purity 99%), 1,4 butanediamine (BDA, purity 98%), ethylene glycol (EG, purity 99%) and choline chloride (ChCl, purity 98%) were purchased from Shanghai Titan Scientific Co. Limited, Nine-Dinn chemistry (Shanghai) Co. Limited, Meryer (Shanghai) chemical technology Co. Limited, Sinopharm chemical reagent Co. Limited, Innochem (Beijing) Co. Limited, Sinopharm chemical reagent Co. Limited and Shanghai Macklin biochemical Co. Limited, respectively. All reagents were directly used without any further treatment. The feed gas composed of 10% CO₂ and 90% N₂ (v/v) was supplied by Air Liquid Co., Limited (Shanghai, China). The gas composition was confirmed through gas chromatography (GC, GC-6600, Shanghai Fanwei Instrument Equipment CO., Limited, China) prior to performing experiments.

The Ni-Cr open cell metal foams were purchased from Taili Metal Work (Suzhou, China). Internal structures of these metal foams were visualized through X-ray microscope Zeiss Xradia 520 Versa from various revolution axes as indicated by Fig. 1, and two distinct images of these metal foams are shown by Fig. S1(Supporting Information). Pore size dataset was generated through random measurement from more than thirty locations as shown by Fig. S2 (Supporting Information). Probability distribution of the pore size dataset was executed through normal, logistic, and lognormal methods, and the lowest standard deviation (0.14) was found by using lognormal distribution, as shown by Fig. S3 (Supporting Information). Table 1 summarizes the structural parameters, such as pore diameter, pore density, porosity, and surface area to volume ratio (m²/m³) of these metal foams. The detailed procedure for evaluation of these parameters by using image processing software Dragonfly Pro is given in the Supporting Information.

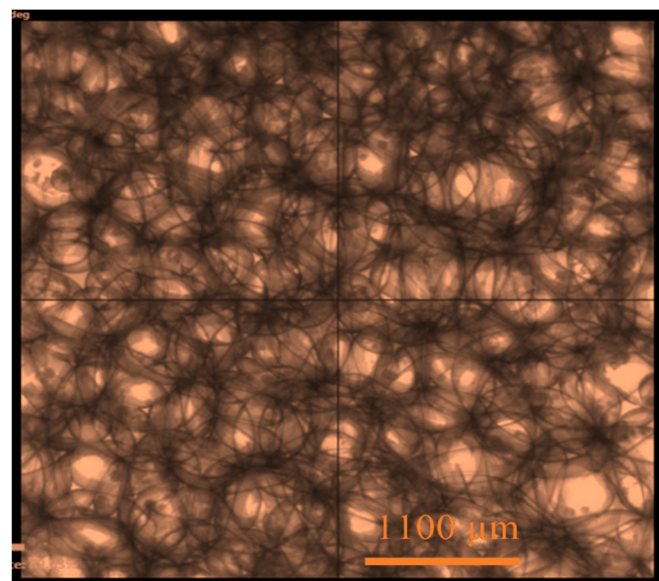


Fig. 1. Ni-Cr Metal foam images obtained from 3D X-ray microscope.

Table 1
Structural parameters of Ni-Cr metal foams (Pasha et al., 2021).

Parameters	Measured Values
Porosity	0.72
Pore size (μm)	145.7
Pore density (ppi)	200
Surface area to volume ratio (m ² /m ³)	1555.6

Table 2

Composition and physical properties of the diamine functionalized DESs.

DES	Hydrogen Bond Acceptor (HBA)	Hydrogen Bond Donor (HBD)	Molar ratio	Diamine used for Functionalization	Molecular weight (g mol ⁻¹)	Viscosity (cP)	Density (g/ml)
DES1	ChCl	EG/HMDA	1:4:1	HMDA	84.1	39.40	1.06
DES2	ChCl	EG/AEEA	1:4:1	AEEA	82.0	63.01	1.15
DES3	ChCl	EG/MAPA	1:4:1	MAPA	79.3	51.13	0.99
DES4	ChCl	EG/EDA	1:4:1	EDA	74.6	32.66	1.08
DES5	ChCl	EG/BDA	1:4:1	BDA	79.3	36.71	1.14

2.2. Synthesis of diamine functionalized deep eutectic solvents

Five diamine functionalized DESs were synthesized according to the method described in several reports (Sarmad et al., 2020; Sze et al., 2014). Firstly, a binary mixture of choline chloride (ChCl) and ethylene glycol (EG) was prepared with a molar ratio of 1:4 under vigorous stirring condition at 80 °C. A large content of EG was selected to reduce the viscosity of this binary mixture. This mixture was naturally cooled to room temperature. Then, it turned into a colorless homogenous liquid after it was dried overnight at 60 °C under vacuum (Sze et al., 2014). HMDA was added into the dried binary mixture for the functionalization, and then the ternary mixture (ChCl: EG: HMDA with the molar ratio of 1:4:1) was heated at 60 °C under vigorous stirring condition. This ternary mixture was termed as HMDA functionalized DES and used for CO₂ absorption in MSRs. Remaining four diamine functionalized DESs were synthesized in a similar way. Physical properties of these DESs are listed in Table 2.

2.3. Characterization of functionalized DESs

¹³C NMR spectra of all functionalized DESs were recorded through Bruker 500 NMR spectrometer with using D₂O solvent before and after CO₂ absorption. Similarly, attenuated total reflectance-Fourier transform infrared (ATR-FTIR) characterization was performed by using Perkin Elmer FTIR spectrometer. ¹³C NMR and ATR-FTIR were typically used to examine the carbamate formation in amine functionalized DES. Thermal stability of all DESs was analyzed by thermogravimetric analysis (TGA), which was executed through TGA-7 of Perkin Elmer. The TGA characterization was performed through heating a DES sample from room temperature to 500 °C

with a rate of 10 °C /min. Viscosities of all DESs before and after CO₂ absorption were monitored through a rotational viscometer (Brookfield, DV2T). Viscosities of some DESs after CO₂ absorption were out of the measurement range of the rotational viscometer, and a Kinexus ultra plus rheometer was used for the viscosity measurement for such specific cases.

2.4. Experimental setup for CO₂ absorption

Detailed description relating to the experimental setup can be viewed from our recent work (Pasha et al., 2021), and it is briefly described here. MSR was predominantly composed of the packed-bed and empty sections that were linked by a connector, as indicated by Fig. 2. Perfluoroalkoxy (PFA) capillaries (Valco Instruments, CO., Limited, United States) were applied to construct these two sections, and the metal foams were inserted in the packed-bed section as suggested in several studies (Sang et al., 2020; Tourville et al., 2015). Both the packed-bed and empty sections of MSR had the same length of 5.0 cm, and their inner diameter was 2.5 mm and 2.0 mm, respectively. The feed gas was stored in a cylinder, and was introduced into the MSR system through a mass flow controller (Beijing Sevenstar Electronics Co., Ltd, China, measuring range:0–500 ml/min) at the volumetric flow rate range of 60–160 ml/min. The diamine functionalized DES was introduced into the MSR system through a piston pump (Scientific system, Inc. USA) at a constant volumetric flow rate of 0.25 ml/min. The temperature of the MSR system was controlled at 40–70 °C through a water bath. A homemade phase separator, fabricated through 3D printer (Formlab form 2), was used for the rapid separation of the gas and liquid phases, which was quite helpful for the elimination of end effects.

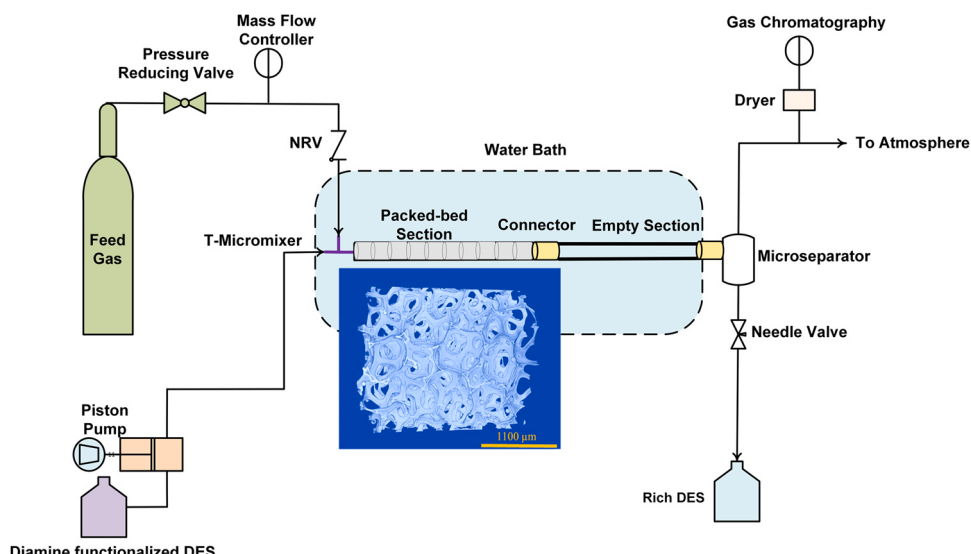
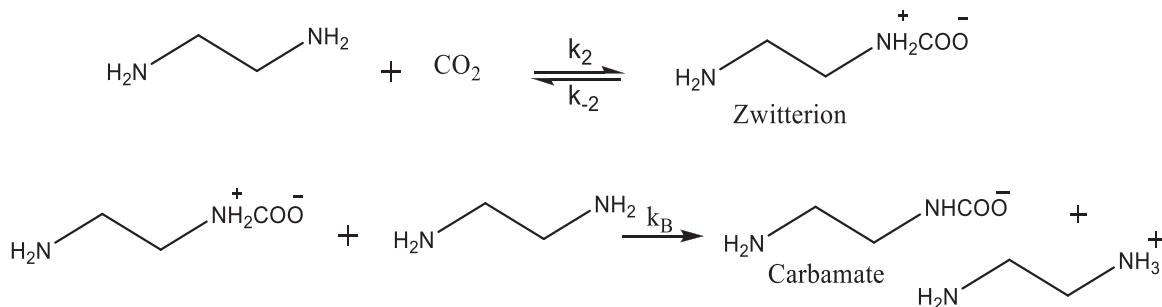
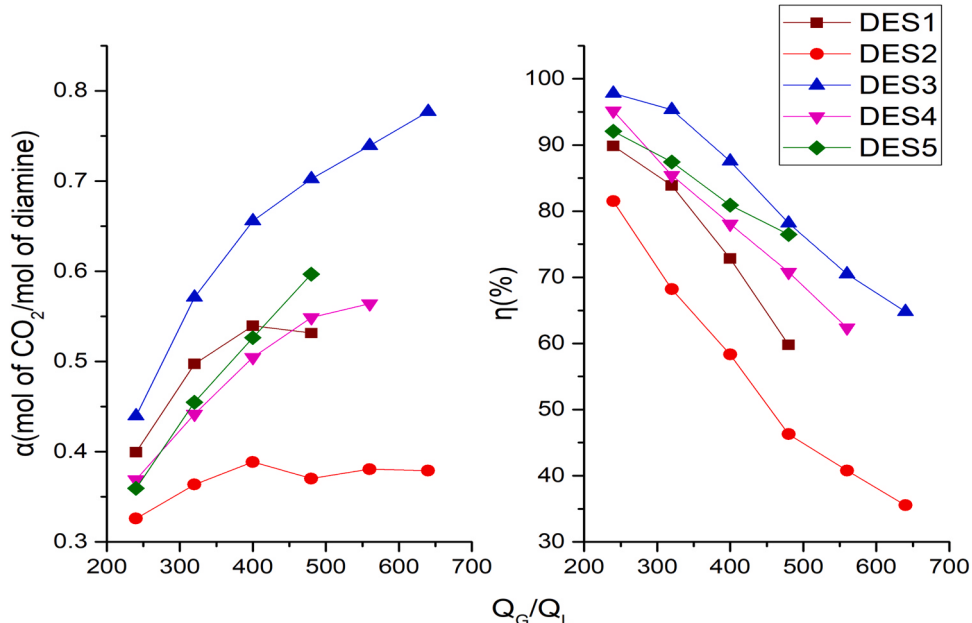


Fig. 2. Schematic diagram of the experimental set-up.

**Scheme 1.** Reaction mechanism for CO₂ absorption by the EDA functionalized DES.**Fig. 3.** CO₂ loading and absorption efficiency of all DESs measured at 40 °C and 1 atm.

Henry constant and overall volumetric mass transfer coefficient could not be determined for this absorption system due to unavailability of equilibrium solubilities of CO₂ in these DESs. Therefore, the absorption performance of all DESs was analyzed by assessing the absorption efficiency (η) and the CO₂ loading (α) by varying the gas to liquid flow rate ratio (Q_G/Q_L) from 240 to 640. These two parameters were based on absorption solubilities and kinetics rate of CO₂ in the involved DESs. All experiments were repeated at least three times under each flow condition, and average values of η and α were finally reported. These two parameters were determined by the following equations:

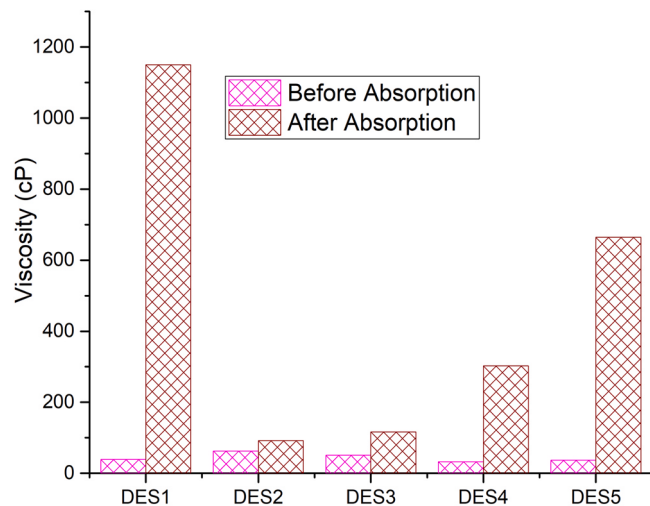
$$\eta = \frac{n_{CO_2in} - n_{CO_2out}}{n_{CO_2in}} \times 100 \quad (1)$$

$$\alpha = \frac{\text{mol of CO}_2}{\text{mol of Diamine}} \quad (2)$$

2.5. Kinetics studies

Amine and superbase functionalized DESs contain amine or imidazolium moiety in HBD or HBA that enables them to chemically react with CO₂, resulting in the formation of carbamate (Haider et al., 2018). Presence of ChCl and EG in the functionalized DESs prepared

in our current work was quite helpful in strengthening the hydrogen bonding interaction with the involved diamines. However, the mixture of ChCl and EG acted as the solvent and diamines mainly

**Fig. 4.** Viscosities of all DESs before and after the CO₂ absorption.

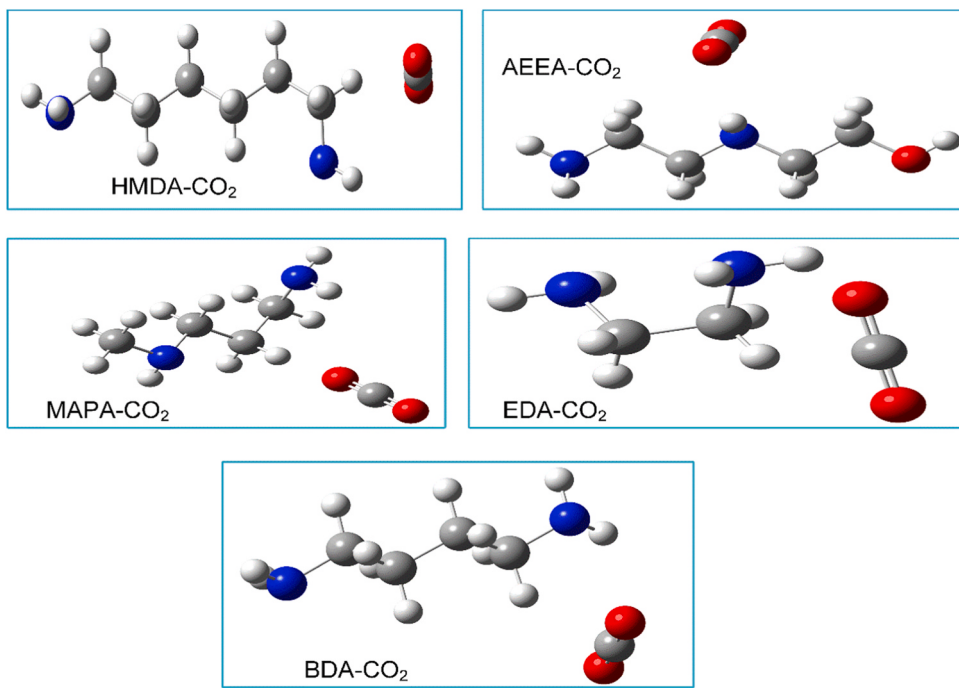


Fig. 5. Optimized structures of diamines and CO₂ in the reactant complexes of these DESs.

participated in chemical absorption, which was confirmed through the ATR-FTIR and ¹³C NMR characterization, as mentioned in [Section 3.1](#). Therefore, the absorption process basically took place through a two-stage zwitterion mechanism. [Scheme 1](#) indicates this reaction mechanism for the CO₂ absorption by the EDA functionalized DES. In the first step, the addition of CO₂ in EDA leads to the zwitterion formation, which is subsequently converted into carbamate through the deprotonation by again reacting with EDA.

In [Scheme 1](#), the parameters k_2 and k_{-2} indicate the rate constants of forward and reverse reactions in the zwitterion formation process, while k_B represents the rate constant of the deprotonation reaction. The reaction mechanism of remaining diamines involved in these diamine functionalized DESs was the same as that of [Scheme 1](#), as the carbamate formation was confirmed through the ¹³C NMR characterization in all DESs, as described in [Section 3.1](#). The zwitterion formation is the rate-determining step and the overall rate of the absorption process is based on the CO₂ concentration, as highlighted in several investigations ([Hartono et al., 2009; Sodiq et al., 2014; Xie et al., 2010](#)). The following kinetic model was used to assess the overall rate constant (k_{ov}).

$$-\frac{dC_{CO_2}}{dt} = k_{ov} C_{CO_2} \quad (3)$$

$$\ln\left(\frac{C_{CO_20}}{C_{CO_2}}\right) = k_{ov} t \quad (4)$$

2.6. Computational studies

Computational studies were carried out to analyze the N–C bond length between the nitrogen atom of amine and the carbon atom of CO₂ during the absorption progress. Reduction in this bond length and movement of proton from amine to CO₂ are the main energy barriers of the zwitterion formation ([Kim et al., 2016](#)). Thus, these effects were determined by optimizing the molecular structures of reactant, transition state and zwitterion complexes for all diamine functionalized DESs. As diamine of each functionalized DES and CO₂ were involved in the chemical reaction thus, they could be considered as a reactant complex, and zwitterion complex is the intermediate in this reaction, as described in [Scheme 1](#). Frequency and geometry optimization of all these structures was executed by using the Gaussian 09 software package with density functional theory (DFT) method and a basis set of B3LYP 6–31 G+(d). Furthermore, integral equation formalism polarizable continuum model (IEF-PCM) was used as a solvation model ([Yamada et al., 2011](#)). Since the molar content of EG was four times higher than ChCl in all DESs, EG with a

Table 3

N–C bond length and O–C–O bond angle in the reactant, transition state and zwitterion complexes.

Diamine-CO ₂ complex	N–C bond length (Å)			O–C–O bond angle		
	Reactant	Transition state	Zwitterion	Reactant	Transition state	Zwitterion
HMDA-CO ₂	4.60	2.15	1.67	180.0	156.1	138.9
AEEA-CO ₂	2.91	2.09	1.68	180.0	153.6	139.1
MAPA-CO ₂	4.29	3.21	1.68	180.0	178.2	139.2
EDA-CO ₂	2.92	2.17	1.34	180.0	156.7	122.3
BDA-CO ₂	5.87	3.22	1.67	180.0	178.2	138.9

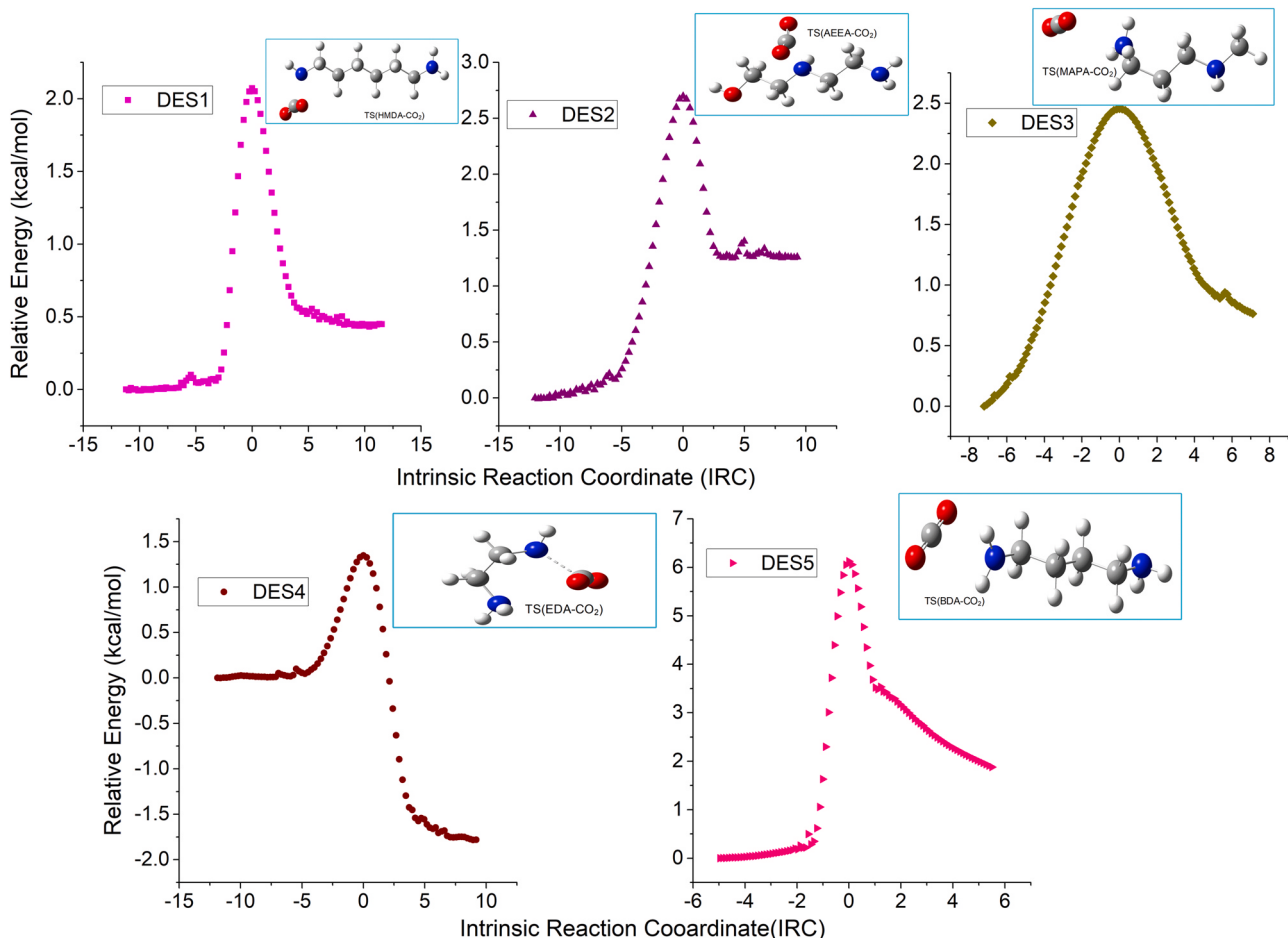


Fig. 6. Intrinsic Reaction Coordinate analysis on the optimized transition structures of diamines and CO₂ used in DES1-DES5.

dielectric constant of 37 was used as the solvent in all computational studies. Moreover, the optimized structures of reactant and zwitterion complexes were verified through zero imaginary frequency and transition state structures were confirmed through at least one imaginary frequency.

3. Results and discussion

3.1. Absorption performance of diamine functionalized DESs

Firstly, the absorption performance in the MSR system was investigated by examining the CO₂ loading (α) and the absorption efficiency (η). Fig. 3 indicates the behavior of these parameters by varying the gas to liquid flow rate ratio, ranging from 240 to 640 in all DESs. DES3 showed the best absorption performance among

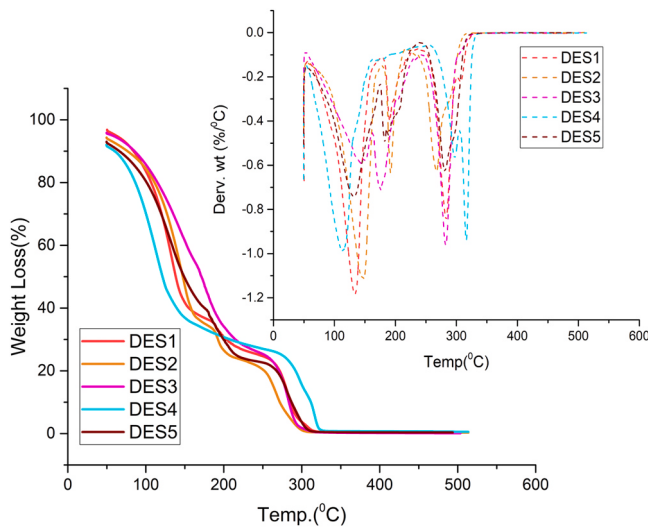


Fig. 7. TGA analysis of the diamine functionalized DESs.

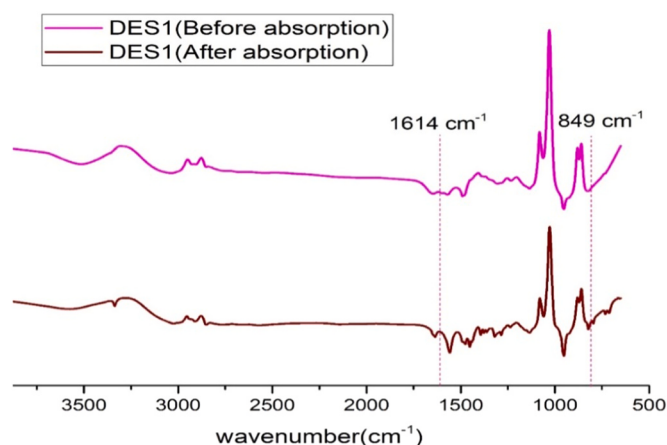


Fig. 8. ATR-FTIR spectra of DES1 before and after the CO₂ absorption.

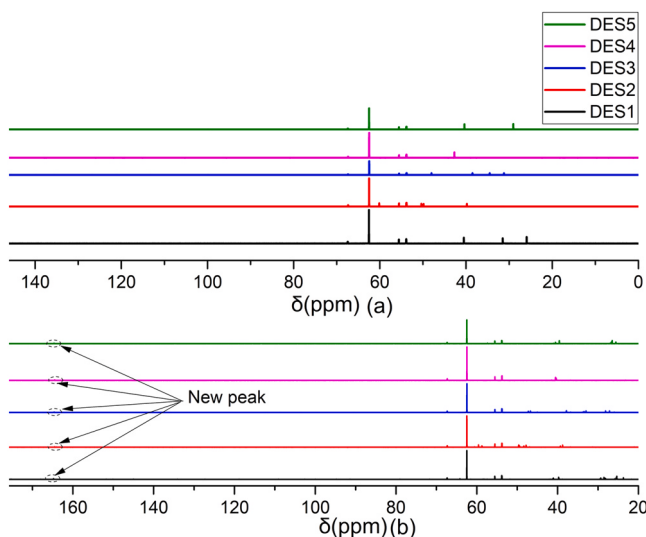


Fig. 9. . ^{13}C NMR spectra of all functionalized DESs (a) before CO_2 absorption (b) after the CO_2 absorption.

these DESs, and the maximum α and η obtained from this DES were approached 0.78 mol of CO_2 / mol of diamine and 98% at the gas to liquid flow rate ratios of 640 and 240, respectively. On the other hand, the CO_2 uptake abilities of DES1, DES4 and DES5 increased linearly with the gas to liquid flow rate ratio in the ranges of 240–400, 240–480 and 240–480, but the abrupt rise in viscosities of these DESs during the progression of CO_2 absorption triggered the solidification of carbamate inside the MSR system and resulted in the clogging issue. Since it was not viable to operate MSR with these DESs under such unsafe and unstable conditions for a longer time duration, the assessment of CO_2 loading was not further extended to high gas to liquid flow rate ratios for these DESs. In contrast, there was a gradual viscosity rise in DES2 and DES3 during the CO_2 absorption at the gas to liquid flow rate ratio of 240–640. However, DES2 showed the lowest absorption performance among these DESs.

The absorption efficiency was dropped by rising the gas to liquid flow rate ratio in all DESs. Reduction of the residence time by the further increase in such high gas to liquid flow rate ratio led to the decrease of axial and radial mass transports (Ye et al., 2013) that triggered the alleviation of η in this MSR system (Lin et al., 2019). A similar trend of the absorption efficiency with the gas to liquid flow rate ratio was found in several other investigations (Ganapathy et al., 2014, 2015).

Rise in the viscosity of a DES due to the CO_2 absorption is a decisive factor to determine its viability for continuous-flow micro-reactors. Fig. 4 indicates the viscosities of these DESs before and after the CO_2 absorption in the MSR system. Initially, DES1, DES4 and DES5 exhibited lower viscosities than DES3, but an opposite trend was found in their viscosities after the CO_2 absorption. In particular, the viscosity rise was quite drastic in DES1 and DES5, as both these diamine functionalized DESs were rapidly transformed into the white solid carbamate due to the CO_2 absorption, subsequently resulting in the clogging of MSR. Conversely, DES3 showed higher CO_2 uptake ability and less increase in the viscosity compared to DES1, DES4 and DES5. It should be noted that the viscosity increase and CO_2 uptake ability of DES3 were 10 times lower and 1.3 times higher than DES1 at the gas to liquid flow rate ratio of 480, respectively. Sharp rise in the viscosities of DES1, DES4 and DES5 did not enable them suitable for the CO_2 absorption in the MSR system at high gas to liquid flow rate ratios. Consequently, these DESs were not used for further investigations in the following sections.

The viscosity rise in these diamine functionalized DESs was compared with the amine and superbase functionalized DESs reported in previous investigations. For instance, Sze et al. (2014) prepared a superbase DES by functionalizing the binary mixture of ChCl and EG with 1,5-diazabicyclo[4.3.0]-non-5-ene (DBN). The viscosity of such a DES after the CO_2 absorption reached 5450 cP, which was much higher than the diamine functionalized DESs prepared in our work. Recently, Sarmad et al. (2020) applied six amine functionalized DESs for CO_2 absorption, and the viscosity of the best performed DES among these amine functionalized DESs reached 650 cP, which was still higher than that of DES3. A high gas to liquid flow ratio was used to examine the absorption performance of MAPA

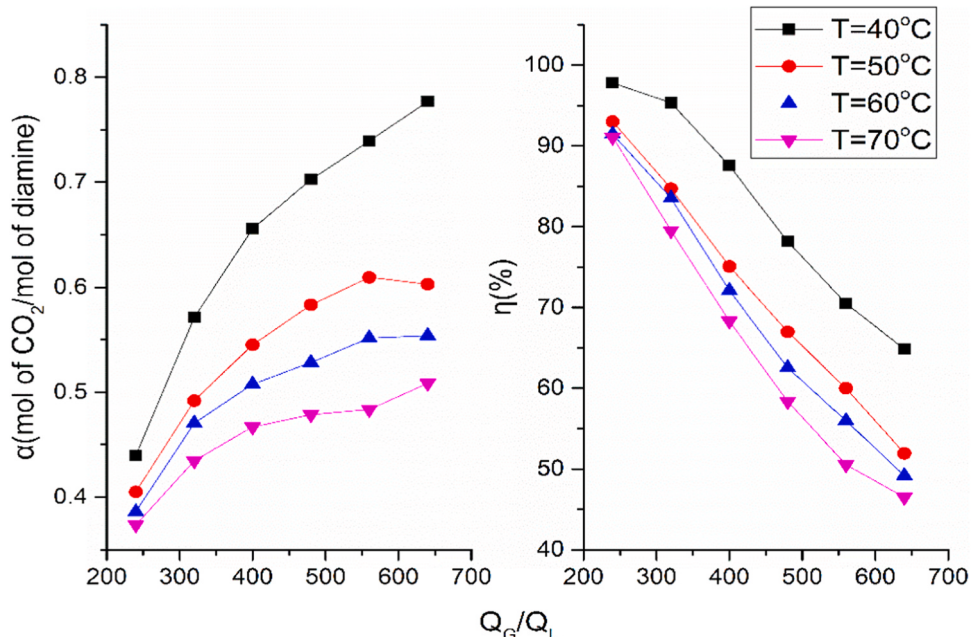


Fig. 10. Influence of temperature on the CO_2 loading and absorption efficiency of DES3.

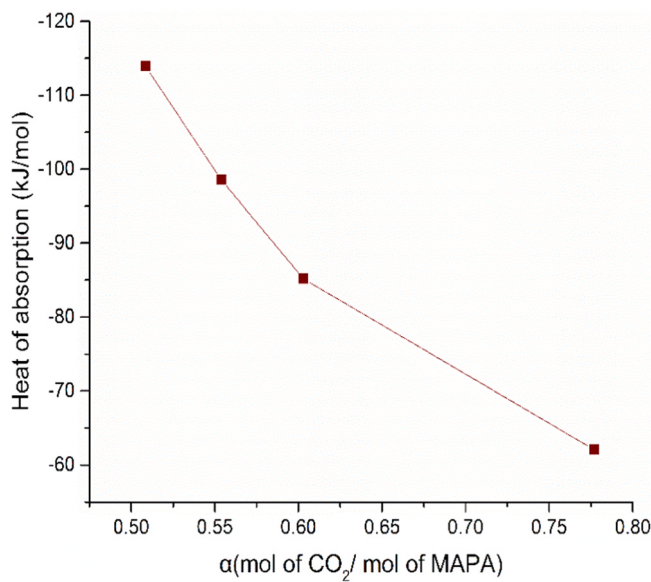


Fig. 11. Heat of absorption of DES3 at the gas to liquid flow rate ratio of 640 and the temperature of 40–70 °C.

functionalized DES (i.e., DES3), but the viscosity rise in this DES was much lower than superbase and amine functionalized DESs used in the aforementioned investigations.

Computational studies were performed to theoretically investigate the energy barrier in the diamine functionalized DESs. Kim et al. (2016) emphasized that the reduction in the N–C bond length and O–C–O bond angle is typically analyzed to evaluate the energy barrier of the zwitterion formation. Since the zwitterion formation is a rate-determining step in the CO_2 absorption process, we evaluated these two structure parameters relating to the reactant, transition state and zwitterion complexes in these diamine functionalized

DESs. In more details, the reactant complex of each DES is composed of its respective diamine and CO_2 molecules, while the zwitterion complex is an intermediate formed in the absorption process (see Scheme 1). Fig. 5 shows the optimized structures of the reactant complexes of these DESs, and Table 3 summarizes the N–C bond length and O–C–O bond angle for the reactant, transition state and zwitterion complexes obtained from their frequency and geometry optimization. The shortest N–C bond length and the smallest O–C–O bond angle were found in the zwitterion complex of the EDA functionalized DES (i.e., DES4). Moreover, the proton transport from amine to CO_2 for the formation of the zwitterion complex was only observed in DES4. Intrinsic reaction coordinate (IRC) analysis on the optimized transition structures was also performed to evaluate the energy barrier, as indicated by Fig. 6. It can be clearly seen that the lowest energy barrier from ground to transition state was found in DES4 with a value of 1.34 kcal/mol. These characteristics could be considered to contribute to the high CO_2 uptake ability of the EDA functionalized DES (DES4). Nevertheless, the sudden rise in the viscosity of DES4 possibly reduced its CO_2 absorption ability compared to the MAPA functionalized DES (DES3) and resulted in the clogging of MSR.

Presence of metal foams in the packed-bed section of MSR was proved to be highly beneficial for improving the CO_2 absorption rate (Pasha et al., 2021). Under such high gas to liquid flow rate ratios (240–640), the gas-liquid two phases were found to form the wavy-annular or annular flow pattern that contained a continuous gas phase as annular core surrounded by thin liquid film. Small pore sizes and tortuous flow paths inside the metal foams triggered larger interfacial contact and high superficial velocities of gas-liquid two phases and resulted in the excellent absorption performance in the MSR system.

Thermal decomposition behavior of DESs is quite different from ILs. In ILs, continuous heating at elevated temperatures leads to the decomposition of cation and anion, but it firstly weakens the hydrogen bonding interaction between HBD and HBA in DESs and later leads to their decomposition (Chen et al., 2018). Appropriate selection of HBD and its content plays a vital role in maintaining the

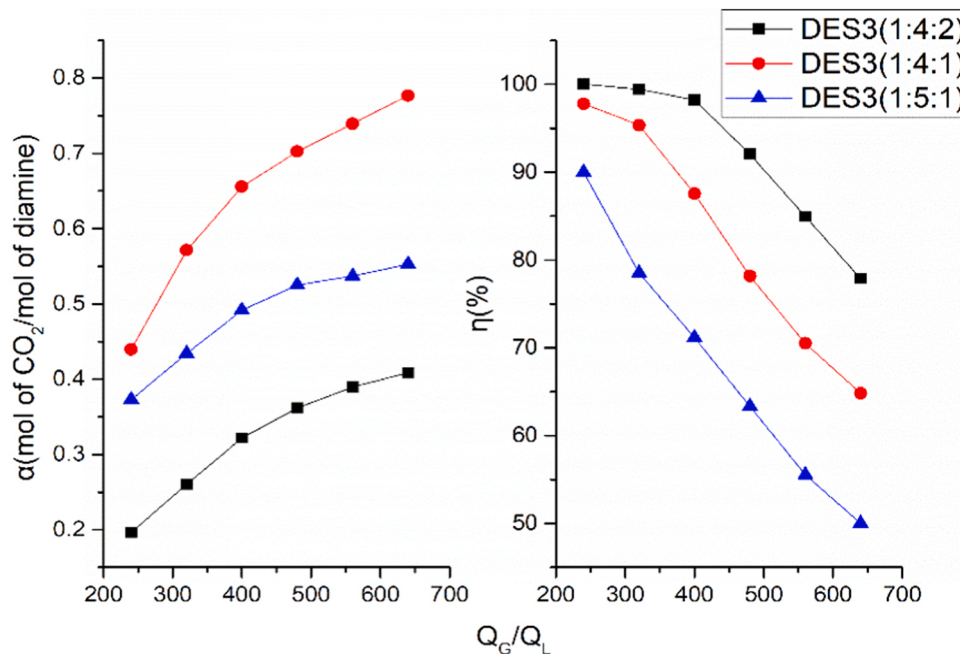


Fig. 12. Influence of the molar ratio of EG to MAPA on the CO_2 loading and absorption efficiency of DES3 (the ratio in the bracket refers to the molar ratio among ChCl, EG and MAPA).

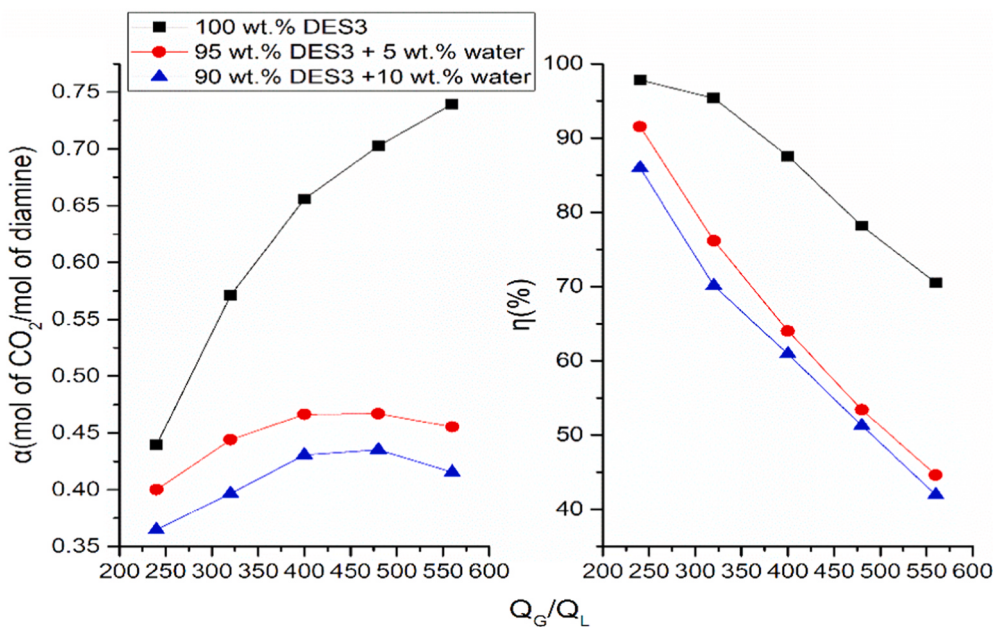


Fig. 13. Influence of water addition on the CO₂ loading and absorption efficiency.

thermal stability of DESs (Sarmad et al., 2020). Fig. 7 indicates the thermal characterization of the diamine functionalized DESs executed through TGA. The decomposition of DESs 1–5 was completed in three steps with the onset temperatures (reflecting 10% weight loss of a DES) of 84.2, 76.5, 85.3, 60.0 and 66.0 °C, respectively. Higher onset temperature of DES3 corresponded to its higher thermal stability compared to the other DESs, which possibly stemmed from stronger hydrogen bonding interaction among MAPA, ChCl and EG.

The ATR-FTIR characterization of DES1 before and after the CO₂ absorption is indicated by Fig. 8. Three important considerations were found in the ATR-FTIR spectra. Firstly, the formation of carbamate was indicated by the appearance of new peaks at 1614 and 854 cm⁻¹, which were ascribed to the νCOO asymmetric stretching and bending (Trivedi et al., 2016). Secondly, there was no peak

observed between 2370 and 2310 cm⁻¹, which reflected the chemical absorption of CO₂ (Gurkan et al., 2010). Lastly, the carbamate formation was indicated by the squeezing of the stretched peak (relating to -NH) centered at 3308 cm⁻¹ in the unreacted DES1 and the appearance of a new peak at 3359 cm⁻¹ in the reacted DES1. Fig. 9 indicates the ¹³C NMR spectra of these functionalized DESs before and after the CO₂ absorption. As shown in Fig. 9(b), for all ¹³C NMR spectra taken after the CO₂ absorption, there was a new peak at 164.77 ppm that corresponded to -NHCOO and represented the formation of carbamate (Trivedi et al., 2016). Moreover, no absorption peak was observed in the range of 123–130 ppm, which corresponded to the chemical absorption of CO₂ (Fu et al., 2021). Therefore, the carbamate formation was confirmed via the ¹³C NMR characterization of all DESs, and details of the chemical shift and peak area of these spectra are provided in the Supporting Information. Since the absorption performance and thermal stability of DES3 were the best among these diamine functionalized DESs, the parametric and kinetic investigations were performed by selecting DES3 in the following sections. Kinetic studies of DES2 were also executed to develop a better performance comparison between DES2 and DES3 under this high gas to liquid flow rate ratio.

3.2. Influence of temperature on the absorption performance of DES3

The rise of temperature (T) has both positive and negative effects on the CO₂ absorption. On the one hand, the increase of temperature leads to the reduction of the DES viscosity promoting the diffusion and mass transport of CO₂. On the other hand, a high temperature shifts the equilibrium of the CO₂ absorption to the reverse direction and expedites the CO₂ desorption (Aghel et al., 2019). Fig. 10 shows the variation of α and η with rising the temperature from 40° to 70°C. Both these parameters significantly dropped with the temperature increase, and the falling trend was strongly influenced by the gas to liquid flow rate ratio. For instance, the CO₂ loading at 40 °C was 1.2 times higher than that of 70 °C at the gas to liquid flow rate ratio of 240, but this difference was more than 1.5 times at the gas to liquid flow rate ratio of 640.

The behavior of the MAPA functionalized DES was quite opposite of aqueous amines. The decrease of the CO₂ uptake ability for this

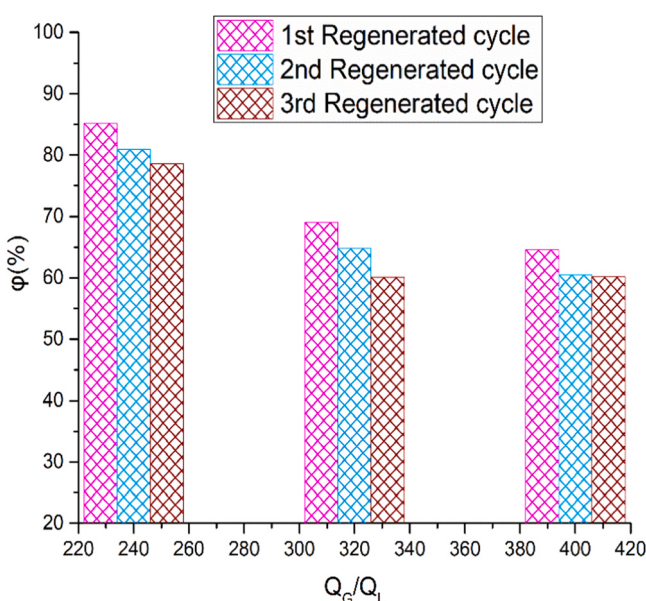


Fig. 14. Regeneration efficiency of DES3 in three consecutive regeneration cycles.

functionalized DES by rising the temperature could be elucidated from the hydrogen bonding interaction between HBD and HBA. D'Agostino et al. (2011) investigated the equilibrium self-diffusion coefficient of choline cation and HBD by using standard stimulated echo pulse field gradient nuclear magnetic resonance (PFG NMR) method. They emphasized that the hydrogen bonding interaction between ChCl and HBD was greatly influenced by the molecular structure of HBD and became weaker by rising the temperature, leading to the reduction in the mobility of cation and anion. Because of this fact, the hydrogen bonding interaction might be reduced among ChCl and EG and MAPA by rising the temperature and resulted in the poor CO₂ absorption performance of DES3. Similar finding was observed in several other studies (Trivedi et al., 2016; Yan et al., 2020; Zhang et al., 2019).

Heat of absorption (ΔH_{abs}) for DES3 was evaluated to examine the energy consumption and regeneration ability of this diamine functionalized DES. Gibbs Helmholtz relationship was selected to evaluate the heat of absorption as this model provides heat of absorption values very close to experimental data (Mathias and O'Connell, 2012; Ramezani et al., 2021; Sobala and Kierzkowska-Pawlak, 2019). It is described by the following equation.

$$\frac{\Delta H_{abs}}{R} = \left(\frac{\partial \ln P_{CO_2}}{\partial (1/T)} \right)_\alpha \quad (5)$$

where the parameters P_{CO_2} , T , ΔH_{abs} and R indicate the partial pressure of CO₂, temperature, heat of absorption and universal gas constant, respectively. We evaluated the heat of absorption of DES3 at the maximum gas to liquid flow rate ratio (640) and the temperature of 40–70 °C, as shown by Fig. 11. It can be clearly seen that the heat of absorption was dropped by rising the CO₂ loading and its lowest value (-62.1 kJ/mol) was found at the highest loading (0.78 mol of CO₂/mol of MAPA) and 40 °C. It should be noted that the heat of absorption of this DES under these conditions was lower than aqueous monoethanolamine (MEA) (-85 kJ/mol at 40 °C) (Kim and S., 2007) and an anion-functionalized ionic liquid (-80 kJ/mol at 25 °C) (Gurkan et al., 2010). Therefore, DES3 could be easily regenerated through mild heating and nitrogen purging, as mentioned in Section 3.5.

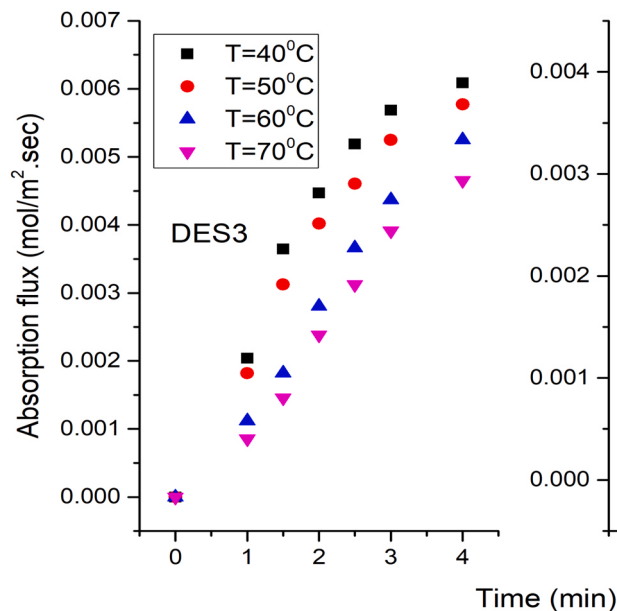


Fig. 15. Absorption flux of DES2 and DES3 evaluated at $Q_G/Q_L = 400$.

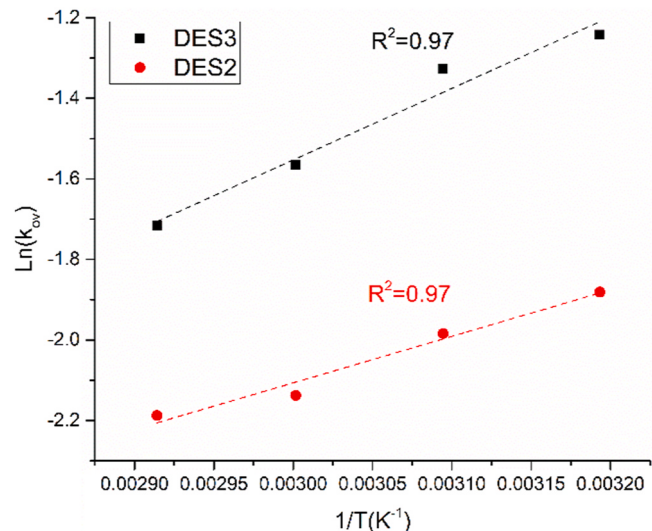
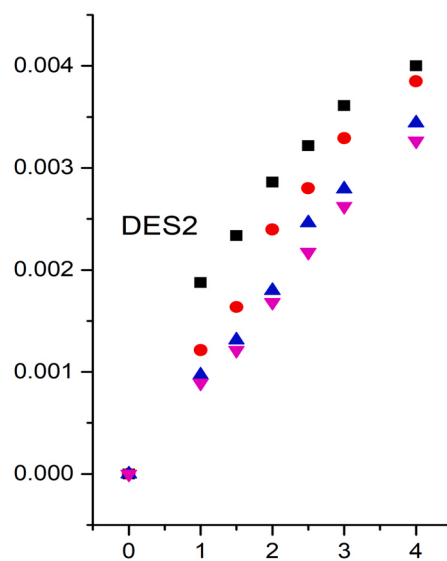


Fig. 16. Arrhenius plot of the kinetic data obtained for DES2 and DES3.

3.3. Influence of HBA to HBD molar ratio on the absorption performance of DES3

Typically, the impact of HBA or HBD concentration on the CO₂ uptake ability of a DES is examined by changing its molar content. However, HBA (i.e., ChCl) is an organic salt and its high concentration possibly leads to the clogging of MSR. Therefore, the analysis on the absorption performance was performed by varying the molar ratio of both HBDs (i.e., EG and MAPA) through the adjustment of their molar amounts while maintaining the same applied molar amount of HBA in DES3. Fig. 12 indicates α and η for DES3 by rising the molar ratio of EG to MAPA. Surprisingly, η rapidly increased, while α drastically dropped with rising the molar ratio of EG to MAPA in DES3. The increase of the MAPA content in



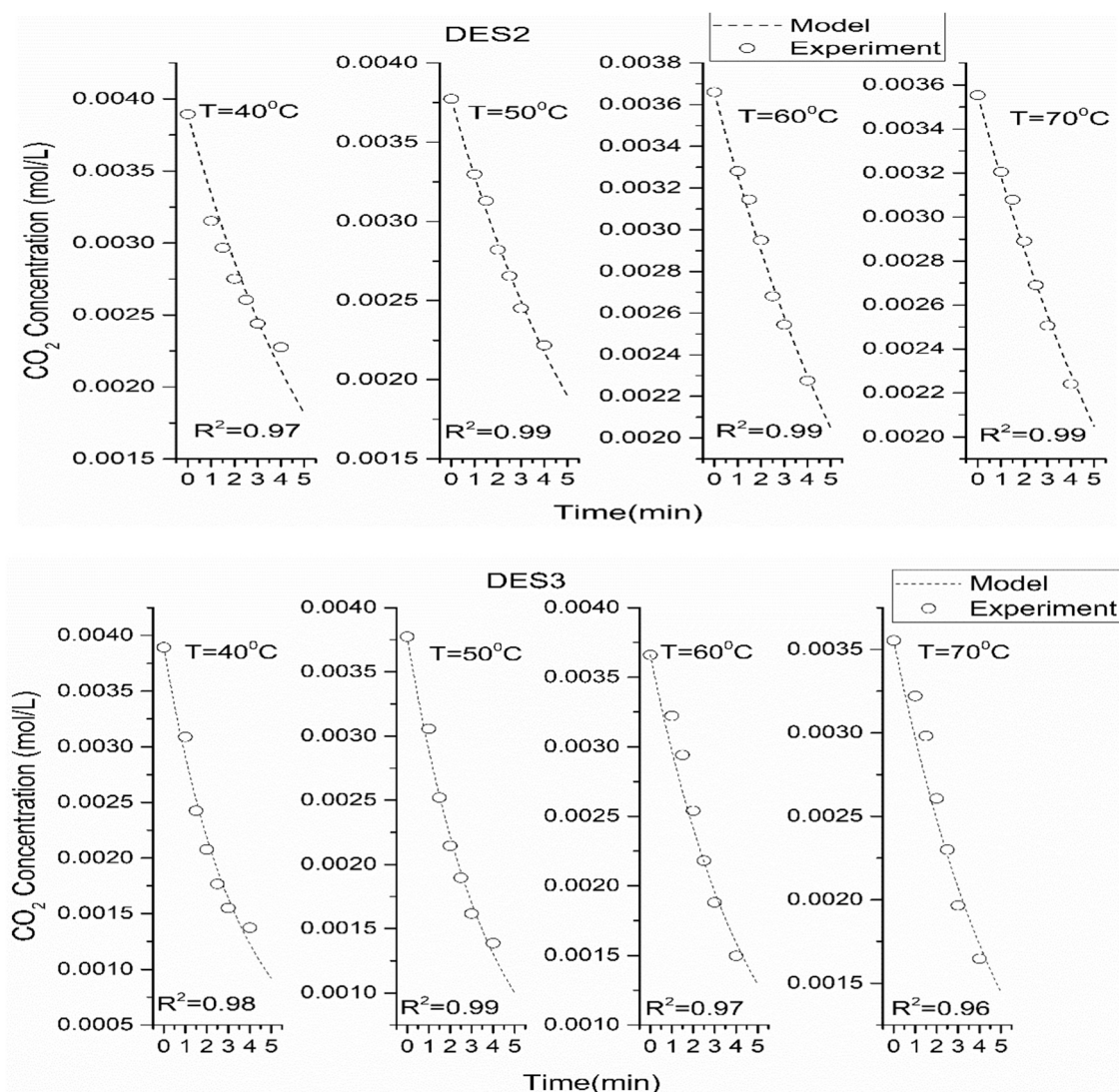


Fig. 17. Experimental and predicated CO_2 concentrations at various residence times with the temperature of 40–70 °C for DES2 and DES3.

DES3 provided larger driving force and faster mobility of ions, stronger hydrogen bonding interaction among HBA and HBDs, and more reactive sites for the CO_2 absorption. However, the CO_2 uptake ability per mole of MAPA was reduced by increasing the molar content of MAPA in DES3. Therefore, it was not feasible to further increase the molar content of MAPA in DES3. The maximum CO_2 loading of DES3 with the 1:4:1 molar ratio among ChCl, EG and MAPA was 0.78 mol of CO_2 / mol of MAPA at the gas to liquid flow rate ratio of 640, which was much higher than the conventional aqueous amines applied for CO_2 absorption in microreactors (Ganapathy et al., 2016; Yao et al., 2017).

Conversely, the rise of the EG molar content in DES3 (e.g., the molar ratio among ChCl, EG and MAPA from 1:4:1–1:5:1) resulted in lowering the CO_2 uptake ability. Basicity and polarizability of EG are much lower than MAPA because of the absence of strong nucleophilic amine moiety. Therefore, the increase in the EG molar content could not possibly provide stronger hydrogen bonding interaction among ChCl, EG and MAPA and led to the decrease in the CO_2 uptake ability. Since the CO_2 uptake ability of DES3 was adversely affected by rising the EG content, the further increase of the EG content seemed to be illogical. Consequently, DES3 with the molar ratio among ChCl, EG and MAPA of 1:4:1 was recommended as an optimal value.

3.4. Influence of water on the absorption performance of DES3

CO_2 absorption performance of DES is greatly influenced by the addition of water. Fig. 13 indicates the behavior of α and η by adding water with 5–10 wt% content in DES3. The CO_2 uptake ability of pure DES3 (without water) sharply increased with rising the gas to liquid flow rate ratio, but the trend showed a declining zone with the addition of water in DES3. Dilution of DES3 with 5 wt% and 10 wt% water respectively decreased its viscosity to 23.4% and 48.2%, which has a favorable impact on the CO_2 absorption to a certain extent. However, it significantly weakens the hydrogen bonding interaction between HBA and HBD, as highlighted in several reports (Gabriele et al., 2019; Ma et al., 2018). Consequently, the absorption performance of DES3 was adversely affected by the water dilution and a similar finding was observed in several other investigations (Fu et al., 2021; Su et al., 2009). Moreover, the water addition not only decreases the CO_2 uptake ability of DES, but also reduces its regeneration ability (Fu et al., 2021).

3.5. Regeneration efficiency of DES

DES regeneration plays a vital role in evaluating the energy requirement for CO_2 absorption processes. Since the heat of absorption

for DES3 was much lower compared to aqueous amines, less energy and shorter time would be required for its regeneration. The regeneration of DES3 was performed by heating the rich DES3 in a glass vial immersed in an oil bath at 80 °C with continuously purging nitrogen for one hour. In contrast, the regeneration of aqueous amine sorbents is typically performed above 100 °C with consistent heating for a longer time duration (Barzaghi et al., 2010; Stowe and Hwang, 2017). The CO₂ loadings in fresh and regenerated sorbents were used to determine the regeneration efficiency (Lv et al., 2015), as given by the following equation:

$$\text{Regeneration efficiency} (\varphi) = \frac{\text{CO}_2 \text{ loading in regenerated DES of } i - \text{cycle}}{\text{CO}_2 \text{ loading in fresh DES}} \quad (6)$$

Fig. 14 shows the regeneration efficiency of DES3 in three consecutive regenerated cycles. It can be clearly seen that the regeneration efficiency of DES3 gradually dropped in subsequent regenerated cycles, and this effect was strongly influenced by the gas to liquid flow rate ratio. It is worth mentioning that the regeneration efficiency of DES3 was significantly high in three cycles at the gas to liquid flow rate ratio of 240, but it drastically decreased in all three cycles at the gas to liquid flow rate ratios of 320 and 400. Moreover, the CO₂ uptake ability of the second or third regenerated DES3 was lower than the first regenerated DES3, which was possibly triggered by the decrease of MAPA concentration in the regenerated cycles. Overall, the best regeneration efficiencies were found to be 85%, 81% and 79% in the first, second and third regenerated cycles at the gas to liquid flow rate ratio 240, respectively. High regeneration and absorption efficiencies were obtained at the gas to liquid flow rate ratio of 240, which could be considered as an optimal value.

3.6. Absorption flux and overall rate constant investigation for DES2 and DES3

This section summarizes the assessment of absorption flux and overall rate constants (k_{ov}) for DES2 and DES3. The absorption performance of DES2 was significantly lower than DES3 as mentioned in Section 3.1 and its kinetics investigation was helpful to better visualize the performance comparison between these DESs and the amine functionalized DESs used in previous studies. The absorption flux was determined by the number of moles of CO₂ absorbed per unit time and effective area of MSR. Fig. 15 shows the absorption flux of both DESs by varying the temperature from 40 to 70 °C. It should be noted that the absorption flux of DES3 was almost 1.5 times of DES2 because of its higher CO₂ uptake ability. Moreover, it sharply decreased by rising temperature for both DESs. The hydrogen bonding interaction among HBA and HBDs became weaker with the increase of the temperature, which possibly reduced the CO₂ absorption rate in both DESs. Finally, these two diamine functionalized

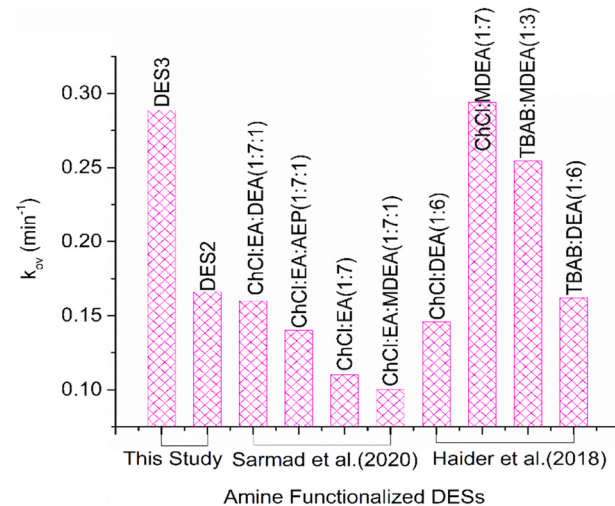


Fig. 18. Comparison of overall rate constants of DES2 and DES3 with the other amine functionalized DESs.

DESs exhibited a linear trend of absorption flux with time prior to reaching the saturation level.

Overall rate constants for the CO₂ absorption by DES2 and DES3 were determined using first-order kinetic model, as indicated by Eq. (4). The slope of this linear model represents k_{ov} , as represented by Fig. S4 (Supporting Information). Fig. 16 indicates the Arrhenius plot for DES2 and DES3. k_{ov} rapidly decreased with the temperature increase in both these diamine functionalized DESs, and the overall rate constant for DES3 was almost 1.6–1.9 times higher than DES2 at the temperature range of 40–70 °C. These values of k_{ov} were used in the overall reaction rate expression indicated by Eq. (3), and CO₂ concentrations were predicted at each temperature by solving kinetic models for both these DESs through ordinary differential equation solver *ode45* in MATLAB. Fig. 17 indicates the predicted and experimental CO₂ concentrations at various residence times with the temperature of 40–70 °C for DES2 and DES3. The R-square value in most cases was ≥ 0.98 , which reflected the good accuracy of this kinetic model.

Fig. 18 indicates the comparison of overall rate constants between these diamine functionalized DESs and the amine functionalized DESs used in previous investigations (Haider et al., 2018; Sarmad et al., 2020). k_{ov} for DES3 obtained at 40 °C was much higher than the amine functionalized DESs used by (Sarmad et al., 2020). They functionalized these DESs by using seven moles of ethanamine (EA) and one additional mole of five different amines per mole of DES, but DES3 functionalized by using only one mole of MAPA per mole of DES and could be applied in microstructured reactors at rather high gas to liquid flow rate ratios. Secondly, k_{ov} for DES3 was

Table 4

Comparison of absorption performance between MSR and other microreactors.

Gas to liquid flow ratio	Microreactor details	Sorbents	Absorption efficiency η (%)	CO ₂ Loading α (mol of CO ₂ /mol of amine) at 10kPa of CO ₂	Regeneration efficiency φ (%)	Reference
1.5–75	Numbered-up (ID = 0.456 mm)	Aqueous DEA	40–99	0.005–0.13	–	(Ganapathy et al., 2016)
0.015–260	Numbered-up	Aqueous DEA	45–97	0.28–0.30	–	(Yao et al., 2017)
4.5–22.75	single Microchannel (ID = 0.254, 0.508, 0.762 mm)	Aqueous DEA	40–99	–	–	(Ganapathy et al., 2015)
18.8–75.2	High-throughput microchannel reactor	MDEA+PZ	25–97	–	–	(Pan et al., 2014)
88.9–666.7	Microstructured reactor	MDEA+ HMDA	23–97	0.10–0.32	65–85	(Pasha et al., 2021)
240–640	Microstructured reactor	DES3	65–98	0.44–0.78	60–85	This study

comparable with the amine functionalized DESs formulated by (Haider et al., 2018). However, they functionalized these DESs by using much larger number of moles of diethanolamine (DEA) and methyldiethanolamine (MDEA) compared to DES3. Overall, DES3 contained less moles of diamine for the functionalization and showed higher k_{ov} than most of previously used amine functionalized DESs at high gas to liquid flow rate ratios.

3.7. Comparison of MSR with other microreactors for CO₂ absorption

In this section, the CO₂ absorption performance in the MSR system with DES3 was compared with previously used micro-reactors. Several key performance indicators, such as absorption efficiency, CO₂ loading, regeneration efficiency and gas to liquid flow rate ratio were used to execute a comprehensive analysis among these various microreactors. The summary of this comparison is presented in Table 4. It is worth noting that the diamine functionalized DES was used for the CO₂ absorption in the current MSR system for the first time, while aqueous amine sorbents were mostly applied for the CO₂ absorption in previous investigations. DES3 exhibited exceptional CO₂ loading and absorption efficiency compared to aqueous amine sorbents at high gas to liquid flow rate ratios due to stronger hydrogen bonding interaction among HBA and HBDs. We used an aqueous mixed amine sorbent composed of 25 wt% MDEA + 5 wt% HMDA (hexamethylenediamine) in the same MSR system according to our recent work (Pasha et al., 2021). However, this sorbent showed much lower CO₂ loading compared to DES3 at identical gas to liquid flow rate ratios. Moreover, the conventional amine sorbents showed larger heat of absorption and higher energy penalty for the regeneration. In contrast, the heat of absorption of DES3 was lower than the conventional amines and anion-functionalized ionic liquids, as mentioned in Section 3.2. Thus, DES3 could be recommended as an energy-efficient and sustainable sorbent for CO₂ capture. In brief, the integration of such an excellent diamine functionalized DES with MSRs having metal foams packings shows great industrial application potential for the CO₂ absorption.

4. Conclusion

Absorption performance of five novel diamine functionalized DESs was investigated in the microstructured reactor (MSR) with metal foams as packing materials at high gas to liquid flow rate ratios. The N-methyl-1,3-propanediamine (MAPA) functionalized DES (DES3) showed excellent CO₂ uptake ability and absorption efficiency without the clogging of MSR. However, the sharp rise in the viscosities of the hexamethylenediamine (HMDA), ethylenediamine (EDA) and 1,4-butanediamine (BDA) functionalized DESs led to the clogging of MSR, and consequently, no further investigation was executed by using these three DESs. Moreover, computational studies indicated that the EDA functionalized DES (DES4) showed the lower energy barrier than DES3, but the sharp rise in its viscosity did not enable this DES to be used for further investigation. Maximum CO₂ loading and absorption efficiency of DES3 reached 0.78 mol of CO₂ / mol of diamine and 98% at the gas to liquid flow rate ratios of 640 and 240, respectively. Besides, optimum molar ratio among ChCl, EG and MAPA in DES3 was found to be 1:4:1, as the further increase in MAPA and EG contents resulted in lowering the CO₂ uptake ability of this DES. However, the absorption performance of DES3 was negatively affected by temperature increase and water dilution.

Heat of absorption for DES3 was significantly lower than conventional amines and anion-functionalized ILs. Likewise, DES3 showed remarkable regeneration efficiency in three consecutive regenerated cycles at the gas to liquid flow rate ratio of 240. Consequently, DES3 could be recommended as an energy-efficient and sustainable sorbent for CO₂ capture. Overall rate constant of the CO₂ absorption for DES3 at 40 °C was higher than most of previously

used amine functionalized DESs at high gas to liquid flow rate ratios. Small pore size and tortuous flow paths inside the metal foams triggered excellent interfacial contact between feed gas and DES3, resulting in the remarkable absorption performance of MSR. Therefore, the unification of this excellent diamine functionalized DES (i.e., DES3) with the microstructured reactors having metal foams in the packed-bed section has a tremendous process intensification potential for the CO₂ capture. We are hopeful that this investigation will inspire the researcher community to develop more functionalized DESs in combination with advanced reactor technology for CO₂ capture.

Declaration of Competing Interest

The authors declare that they have no known competing financial interests or personal relationships that could have appeared to influence the work reported in this paper.

Acknowledgements

We acknowledge gratefully the financial supports for the project from the National Natural Science Foundation of China (No. 21676164), Science and Technology Commission of Shanghai Municipality (No: 18520743500) and the Shanghai Jiao Tong University Scientific and Technological Innovation Funds (No: 2019QYB06).

Appendix A. Supporting information

Supplementary data associated with this article can be found in the online version at doi:10.1016/j.psep.2021.12.043.

References

- Abbott, A.P., Boothby, D., Capper, G., Davies, D.L., Rasheed, R.K., 2004. Deep eutectic solvents formed between choline chloride and carboxylic acids: versatile alternatives to ionic liquids. *J. Am. Chem. Soc.* 126, 9142–9147.
- Aghaie, M., Rezaei, N., Zendehboudi, S., 2018. A systematic review on CO₂ capture with ionic liquids: current status and future prospects. *Renew. Sustain. Energy Rev.* 96, 502–525.
- Aghel, B., Heidaryan, E., Sahraie, S., Mir, S., 2019. Application of the microchannel reactor to carbon dioxide absorption. *J. Clean. Prod.* 231, 723–732.
- Altamash, T., Atilhan, M., Aliyan, A., Ullah, R., García, G., Aparicio, S., 2016. Insights into choline chloride–phenylacetic acid deep eutectic solvent for CO₂ absorption. *RSC Adv.* 6, 109201–109210.
- Barzaghi, F., Mani, F., Peruzzini, M., 2010. Continuous cycles of CO₂ absorption and amine regeneration with aqueous alkanolamines: a comparison of the efficiency between pure and blended DEA, MDEA AMP Solut. 13C. NMR Spectrosc. Energy Environ. Sci. 3, 772–779.
- Carriazo, D., Serrano, M.C., Gutiérrez, M.C., Ferrer, M.L., del Monte, F., 2012. Deep-eutectic solvents playing multiple roles in the synthesis of polymers and related materials. *Chem. Soc. Rev.* 41, 4996–5014.
- Chen, W., Xue, Z., Wang, J., Jiang, J., Zhao, X., Mu, T., 2018. Investigation on the thermal stability of deep eutectic solvents. *Acta Phys. Chim. Sin.* 34, 904–911.
- D'Agostino, C., Harris, R.C., Abbott, A.P., Gladden, L.F., Mantle, M.D., 2011. Molecular motion and ion diffusion in choline chloride based deep eutectic solvents studied by ¹H pulsed field gradient NMR spectroscopy. *Phys. Chem. Chem. Phys.* 13, 21383–21391.
- Drage, T.C., Snape, C.E., Stevens, L.A., Wood, J., Wang, J., Cooper, A.I., Dawson, R., Guo, X., 2012. Step Change Adsorbents and Processes for CO₂ Capture “STEPCAP”. In: Aroussi, A., Benyahia, F. (Eds.), *Proceedings of the 3rd Gas Processing Symposium*. Elsevier, Oxford, pp. 30–37.
- Dutcher, B., Fan, M., Russell, A.G., 2015. Amine-based CO₂ capture technology development from the beginning of 2013—a review. *ACS Appl. Mater. Interfaces* 7, 2137–2148.
- Fu, H., Wang, X., Sang, H., Liu, J., Lin, X., Zhang, L., 2021. Highly efficient absorption of carbon dioxide by EG-assisted DBU-based deep eutectic solvents. *J. CO₂ Util.* 43, 101372.
- Gabriele, F., Chiarini, M., Germani, R., Tiecco, M., Spreti, N., 2019. Effect of water addition on choline chloride/glycol deep eutectic solvents: characterization of their structural and physicochemical properties. *J. Mol. Liq.* 291, 111301.
- Ganapathy, H., Shooshtari, A., Dessiatoun, S., Alshehhi, M., Ohadi, M., 2014. Fluid flow and mass transfer characteristics of enhanced CO₂ capture in a minichannel reactor. *Appl. Energy* 119, 43–56.
- Ganapathy, H., Shooshtari, A., Dessiatoun, S., Ohadi, M., Alshehhi, M., 2015. Hydrodynamics and mass transfer performance of a microreactor for enhanced gas separation processes. *Chem. Eng. J.* 266, 258–270.

- Ganapathy, H., Steinmayer, S., Shooshtari, A., Dessiatoun, S., Ohadi, M.M., Alshehhi, M., 2016. Process intensification characteristics of a microreactor absorber for enhanced CO₂ capture. *Appl. Energy* 162, 416–427.
- Guo, R., Fu, T., Zhu, C., Yin, Y., Ma, Y., 2019. Hydrodynamics and mass transfer of gas-liquid flow in a tree-shaped parallel microchannel with T-type bifurcations. *Chem. Eng. J.* 373, 1203–1211.
- Gurkan, B.E., de la Fuente, J.C., Mindrup, E.M., Ficke, L.E., Goodrich, B.F., Price, E.A., Schneider, W.F., Brennecke, J.F., 2010. Equimolar CO₂ absorption by anion-functionalized ionic liquids. *J. Am. Chem. Soc.* 132, 2116–2117.
- Haider, M.B., Jha, D., Marriyappan Sivagnanam, B., Kumar, R., 2018. Thermodynamic and kinetic studies of CO₂ capture by glycol and amine-based deep eutectic solvents. *J. Chem. Eng. Data* 63, 2671–2680.
- Hansen, B.B., Spittle, S., Chen, B., Poe, D., Zhang, Y., Klein, J.M., Horton, A., Adhikari, L., Zelovich, T., Doherty, B.W., Gurkan, B., Maginn, E.J., Ragauskas, A., Dadmun, M., Zawodzinski, T.A., Baker, G.A., Tuckerman, M.E., Savinell, R.F., Sangoro, J.R., 2021. Deep eutectic solvents: a review of fundamentals and applications. *Chem. Rev.* 121, 1232–1285.
- Hartono, A., da Silva, E.F., Svendsen, H.F., 2009. Kinetics of carbon dioxide absorption in aqueous solution of diethylenetriamine (DETA). *Chem. Eng. Sci.* 64, 3205–3213.
- Kim, I., S, H., 2007. Heat of absorption of carbon dioxide (CO₂) in monoethanolamine (MEA) and 2-(Aminoethyl)ethanolamine (AEEA) solutions. *Ind. Eng. Chem. Res.* 46, 5803–5809.
- Kim, S., Shi, H., Lee, J.Y., 2016. CO₂ absorption mechanism in amine solvents and enhancement of CO₂ capture capability in blended amine solvent. *Int. J. Greenh. Gas. Control* 45, 181–188.
- Lim, X., 2015. How to make the most of carbon dioxide. *Nat. N.* 526, 628–630.
- Lin, G., Jiang, S., Zhu, C., Fu, T., Ma, Y., 2019. Mass-transfer characteristics of CO₂ absorption into aqueous solutions of n-methyldiethanolamine+ diethanolamine in a t-junction microchannel. *ACS Sustain. Chem. Eng.* 7, 4368–4375.
- Lv, B., Shi, Y., Sun, C., Liu, N., Li, W., Li, S., 2015. CO₂ capture by a highly-efficient aqueous blend of monoethanolamine and a hydrophilic amino acid ionic liquid [C2OHmim][Gly]. *Chem. Eng. J.* 270, 372–377.
- Ma, C., Laaksonen, A., Liu, C., Lu, X., Ji, X., 2018. The peculiar effect of water on ionic liquids and deep eutectic solvents. *Chem. Soc. Rev.* 47, 8685–8720.
- Ma, D., Zhu, C., Fu, T., Yuan, X., Ma, Y., 2020. An effective hybrid solvent of MEA/DEEA for CO₂ absorption and its mass transfer performance in microreactor. *Sep. Purif. Technol.* 242, 116795.
- Mathias, P.M., O'Connell, J.P., 2012. The gibbs-helmholtz equation and the thermodynamic consistency of chemical absorption data. *Ind. Eng. Chem. Res.* 51, 5090–5097.
- Nguyen, T.B.H., Zondervan, E., 2018. Ionic liquid as a selective capture method of CO₂ from different sources: comparison with MEA. *ACS Sustain. Chem. Eng.* 6, 4845–4853.
- Pan, M.-Y., Qian, Z., Shao, L., Arowo, M., Chen, J.-F., Wang, J.-X., 2014. Absorption of carbon dioxide into N-methyldiethanolamine in a high-throughput microchannel reactor. *Sep. Purif. Technol.* 125, 52–58.
- Pasha, M., Li, G., Shang, M., Liu, S., Su, Y., 2021. Mass transfer and kinetic characteristics for CO₂ absorption in microstructured reactors using an aqueous mixed amine. *Sep. Purif. Technol.* 274, 118987.
- Ramdin, M., de Loos, T.W., Vlugt, T.J., 2012a. State-of-the-art of CO₂ capture with ionic liquids. *Ind. Eng. Chem. Res.* 51, 8149–8177.
- Ramdin, M., de Loos, T.W., Vlugt, T.J.H., 2012b. StAtE-of-the-art of CO₂ Capture With Ionic Liquids. *Ind. Eng. Chem. Res.* 51, 8149–8177.
- Ramezani, R., Mazinan, S., Di Felice, R., 2021. Density, viscosity, pH, heat of absorption, and CO₂ Loading Capacity Of Methyl-diethanolamine And Potassium Lysinate Blend Solutions. *J. Chem. Eng. Data* 66, 1611–1629.
- Sang, L., Tu, J., Cheng, H., Luo, G., Zhang, J., 2020. Hydrodynamics and mass transfer of gas-liquid flow in micropacked bed reactors with metal foam packing. *AIChE J.* 66, e16803.
- Sarmad, S., Mikkola, J.-P., Ji, X., 2017. Carbon dioxide capture with ionic liquids and deep eutectic solvents: a new generation of sorbents. *ChemSusChem* 10, 324–352.
- Sarmad, S., Nikjoo, D., Mikkola, J.-P., 2020. Amine functionalized deep eutectic solvent for CO₂ capture: Measurements and modeling. *J. Mol. Liq.* 309, 113159.
- Smith, E.L., Abbott, A.P., Ryder, K.S., 2014. Deep eutectic solvents (DESs) and their applications. *Chem. Rev.* 114, 11060–11082.
- Sobala, K., Kierzkowska-Pawlak, H., 2019. Heat of absorption of CO₂ in aqueous N,N-diethylethanolamine + N-methyl-1,3-propanediamine solutions at 313 K. *Chin. J. Chem. Eng.* 27, 628–633.
- Sodiq, A., Rayer, A.V., Olanrewaju, A.A., Abu Zahra, M.R.M., 2014. Reaction kinetics of carbon dioxide (CO₂) absorption in sodium salts of taurine and proline using a stopped-flow technique. *Int. J. Chem. Kinet.* 46, 730–745.
- Stowe, H.M., Hwang, G.S., 2017. Fundamental understanding of CO₂ capture and regeneration in aqueous amines from first-principles studies: recent progress and remaining challenges. *Ind. Eng. Chem. Res.* 56, 6887–6899.
- Su, W.C., Wong, D.S.H., Li, M.H., 2009. Effect of water on solubility of carbon dioxide in (aminomethanamide + 2-Hydroxy-N,N,N-trimethylethanaminium chloride). *J. Chem. Eng. Data* 54, 1951–1955.
- Sun, C., Wen, S., Zhao, J., Zhao, C., Li, W., Li, S., Zhang, D., 2017. Mechanism and kinetics study of CO₂ absorption into blends of N-methyldiethanolamine and 1-hydroxyethyl-3-methylimidazolium glycine aqueous solution. *Energy Fuels* 31, 12425–12433.
- Sze, L.L., Pandey, S., Ravula, S., Pandey, S., Zhao, H., Baker, G.A., Baker, S.N., 2014. Ternary deep eutectic solvents tasked for carbon dioxide capture. *ACS Sustain. Chem. Eng.* 2, 2117–2123.
- Tourvieille, J.-N., Philippe, R., de Bellefon, C., 2015. Milli-channel with metal foams under an applied gas-liquid periodic flow: flow patterns, residence time distribution and pulsing properties. *Chem. Eng. Sci.* 126, 406–426.
- Trivedi, T.J., Lee, J.H., Lee, H.J., Jeong, Y.K., Choi, J.W., 2016. Deep eutectic solvents as attractive media for CO₂ capture. *Green. Chem.* 18, 2834–2842.
- Uma Maheswari, A., Palanivelu, K., 2015. Carbon dioxide capture and utilization by alkanolamines in deep eutectic solvent medium. *Ind. Eng. Chem. Res.* 54, 11383–11392.
- Vishwakarma, N.K., Singh, A.K., Hwang, Y.-H., Ko, D.-H., Kim, J.-O., Babu, A.G., Kim, D.-P., 2017. Integrated CO₂ capture-fixation chemistry via interfacial ionic liquid catalyst in laminar gas/liquid flow. *Nat. Commun.* 8, 14676.
- Xie, H.-B., Zhou, Y., Zhang, Y., Johnson, J.K., 2010. Reaction mechanism of monoethanolamine with co₂ in aqueous solution from molecular modeling. *J. Phys. Chem. A* 114, 11844–11852.
- Yamada, H., Matsuzaki, Y., Higashii, T., Kazama, S., 2011. Density functional theory study on carbon dioxide absorption into aqueous solutions of 2-Amino-2-methyl-1-propanol using a continuum solvation model. *J. Phys. Chem. A* 115, 3079–3086.
- Yan, H., Zhao, L., Bai, Y., Li, F., Dong, H., Wang, H., Zhang, X., Zeng, S., 2020. Superbase ionic liquid-based deep eutectic solvents for improving CO₂ absorption. *ACS Sustain. Chem. Eng.* 8, 2523–2530.
- Yao, C., Zhu, K., Liu, Y., Liu, H., Jiao, F., Chen, G., 2017. Intensified CO₂ absorption in a microchannel reactor under elevated pressures. *Chem. Eng. J.* 319, 179–190.
- Ye, C., Dang, M., Yao, C., Chen, G., Yuan, Q., 2013. Process analysis on CO₂ absorption by monoethanolamine solutions in microchannel reactors. *Chem. Eng. J.* 225, 120–127.
- Zhang, N., Huang, Z., Zhang, H., Ma, J., Jiang, B., Zhang, L., 2019. Highly efficient and reversible CO₂ capture by task-specific deep eutectic solvents. *Ind. Eng. Chem. Res.* 58, 13321–13329.
- Zhang, Q., De Oliveira Vigier, K., Royer, S., Jérôme, F., 2012. Deep eutectic solvents: syntheses, properties and applications. *Chem. Soc. Rev.* 41, 7108–7146.